A long noncoding (lnc)RNA governs expression of the phosphate transporter Pho84 in fission yeast and has cascading effects on the flanking *prt* lncRNA and *pho1* genes

Received for publication, December 7, 2017, and in revised form, January 16, 2018 Published, Papers in Press, February 2, 2018, DOI 10.1074/jbc.RA117.001352

Angad Garg[‡], **Ana M. Sanchez**[§], **Stewart Shuman**[‡1], **and Beate Schwer**[§2]

From the [‡]*Molecular Biology Program, Sloan-Kettering Institute, New York and the* [§]*Department of Microbiology and Immunology, Weill Cornell Medical College, New York, New York 10065*

Edited by Charles E. Samuel

The expression of the phosphate transporter Pho84 in fission yeast *Schizosaccharomyces pombe* is repressed in phosphate-rich medium and induced during phosphate starvation. Two other phosphate-responsive genes in *S. pombe* (*pho1* and *tgp1*) had been shown to be repressed in *cis* by transcription of a long noncoding (lnc) RNA from the upstream flanking gene, but whether *pho84* expression is regulated in this manner is unclear. Here, we show that repression of *pho84* is enforced by transcription of the SPBC8E4.02c locus upstream of *pho84* to produce a lncRNA that we name *prt2* (*pho*-repressive transcript 2). We identify two essential elements of the *prt2* promoter, a HomolD box and a TATA box, mutations of which inactivate the *prt2* promoter and de-repress the downstream *pho84* promoter under phosphate-replete conditions. We find that *prt2* promoter inactivation also elicits a cascade effect on the adjacent downstream *prt* (lncRNA) and *pho1* (acid phosphatase) genes, whereby increased *pho84* transcription down-regulates *prt* lncRNA transcription and thereby de-represses *pho1*. Our results establish a unified model for the repressive arm of fission yeast phosphate homeostasis, in which transcription of *prt2*, *prt*, and *nc-tgp1* lncRNAs interferes with the promoters of the flanking *pho84*, *pho1*, and *tgp1* genes, respectively.

Fungi respond to phosphate starvation by inducing the transcription of phosphate acquisition genes (1). The phosphate regulon in the fission yeast *Schizosaccharomyces pombe* comprises three genes that specify, respectively, a cell-surface acid phosphatase Pho1, an inorganic phosphate transporter Pho84, and a glycerophosphate transporter Tgp1 (2). Expression of *pho1* and *tgp1* is actively repressed during growth in phosphate-rich medium by the transcription in *cis* of a long noncoding (lnc)[3] RNA from the 5′-flanking genes *prt* and *nc-tgp1* (3–8). The *prt* lncRNA initiates 1147 nucleotides (nt) upstream of the *pho1* mRNA transcription start site (Fig. 1*A*). The *nc-tgp1* lncRNA initiates 1823 nt upstream of the *tgp1* mRNA start site.

pho1 expression from the *prt-pho1* locus and *tgp1* expression from the *nc-tgp1-tgp1* locus are both inversely correlated with the activity of the lncRNA promoters. Transcription of the *prt* and *nc-tgp1* lncRNAs is driven by distinctive bi-partite promoters, consisting of a HomolD box and a TATA box located sequentially within a 100-nt segment preceding the start sites (6, 8). Mutations in the HomolD and TATA boxes of the *prt* or *nc-tgp1* genes result in de-repression of the downstream *pho1* or *tgp1* promoters in phosphate-replete cells. The ensuing synthesis of the *pho1* and *tgp1* mRNAs (as well as their induction during phosphate starvation) depends on the DNA-binding transcription factor Pho7 (2, 9), which recognizes a 12-nt sequence motif (5′-TCG(G/C)(A/T)*XX*TT*X*AA) present in the *pho1* and *tgp1* promoters (10). A simple model for the repressive arm of fission yeast phosphate homeostasis is that transcription of the upstream lncRNA interferes with expression of the downstream genes encoding Pho1 or Tgp1 by displacing Pho7 from the *pho1* and *tgp1* promoters (6–8).

The basal level of *pho1* expression is also governed by the phosphorylation state of the carboxyl-terminal domain (CTD) of the Rpb1 subunit of RNA polymerase II (pol II). For example, CTD mutations that prevent installation of the Ser7-PO_4 or Ser5-PO_4 marks de-repress *pho1* in phosphate-replete cells. By contrast, prevention of the Thr4-PO_4 mark hyper-represses *pho1* under phosphate-rich conditions (5). Because such CTD mutations do not affect the activity of the *prt* or *pho1* promoters *per se*, it is proposed that CTD status affects pol II termination during *prt* lncRNA synthesis and thus the propensity to displace Pho7 from the *pho1* promoter (6). Absence of CTD Ser7-PO_4 or limitation of Ser5-PO_4 elicits a similar de-repression of transcription from the *tgp1* promoter in phosphate-replete cells, without affecting the activity of the *nc-tgp1* promoter (8). *tgp1* de-repression by limiting Ser5-PO_4 entails a switch in *nc-tgp1* poly(A) site utilization to generate a short *nc-tgp1* RNA that does not interfere with the *tgp1* promoter (8).

The third gene in the fission yeast phosphate regulon, *pho84*, is situated immediately upstream of the *prt-pho1* locus (Fig. 1*A*). Previously, we mapped the 5′ ends of the *pho84* mRNA to a pair of sites located 151 and 149 nt upstream of the start codon of the *pho84* open reading frame (Fig. 1*A*) (5). We noted concordant effects of CTD phospho-site mutations on the levels of

This work was supported by National Institutes of Health Grant GM52470 (to S. S. and B. S.). The authors declare that they have no conflicts of interest with the contents of this article. The content is solely the responsibility of the authors and does not necessarily represent the official views of the National Institutes of Health.

This article contains Figs. S1 and S2.

[1] To whom correspondence may be addressed. Tel.: 212-639-7145; E-mail: s-shuman@ski.mskcc.org.

[2] To whom correspondence may be addressed. Tel.: 212-746-6518; E-mail: bschwer@med.cornell.edu.

[3] The abbreviations used are: lncRNA, long noncoding RNA; nt, nucleotide; DBD, DNA-binding domain; CTD, carboxyl-terminal domain; pol, polymerase; PAS, polyadenylation signal; RACE, rapid amplification of cDNA ends.

pho1 and *pho84* mRNAs in phosphate-replete cells (5). Also, the induction of both *pho1* and *pho84* during phosphate starvation was delayed in *rrp6*Δ cells that accumulate high levels of *prt* lncRNA (5). These results raised the prospect that the *prt* lncRNA might act as a repressor of both upstream and downstream protein-coding genes. Alternatively, there could be another regulatory RNA, distinct from *prt* but also increased in *rrp6*Δ cells, that controls *pho84* expression.

Here, we report that the latter model is correct. We find that the fission yeast SPBC8E4.02c gene located upstream of *pho84* (Fig. 1*A*) specifies a lncRNA that represses *pho84* expression. We named this locus *prt2* (*pho*-repressive transcript 2). Here, we characterize the *prt2* lncRNA, define the *prt2* promoter, and show that inactivation of the *prt2* promoter up-regulates the *pho84* promoter in phosphate-replete cells. We describe a cascade effect of *prt2* promoter inactivation on the downstream *prt-pho1* locus, whereby increased *pho84* transcription down-regulates *prt* and thereby de-represses *pho1*.

Results

Characterization of a prt2 lncRNA initiating from the SPBC8E4.02c locus

Given the precedents of *prt* and *nc-tgp1* lncRNAs regulating their 3′-flanking protein-coding genes, we inspected the genomic region upstream of *pho84* as a potential source of a candidate *pho84*-regulatory RNA. As annotated in PomBase (www.pombase.org),[4] the *pho84* gene is flanked by a co-oriented gene SPBC8E4.02c (Fig. 1*A*), spanning 1618 nt and abutting the 5′ end of *pho84*. In the center of the SPBC8E4.02c locus is a 387-nt ORF (indicated by the *arrow* in Fig. 1*A*) with the potential to encode a 129-amino acid polypeptide, annotated as an "uncharacterized *S. pombe*-specific protein." Our search of the NCBI database retrieved no hits, even from closely related species in the genus *Schizosaccharomyces*. The lack of homology, and the presence of upstream AUG elements in the putative 5′-UTR, led us to suspect that SPBC8E4.02c is not a coding gene. Our hypothesis was that SPBC8E4.02c specifies a lncRNA with a regulatory function *vis à vis pho84*, akin to how *prt* regulates *pho1*. Thus, we designated the SPBC8E4.02c gene as *prt2*.

Northern analysis of total RNA from logarithmically growing phosphate-replete wildtype *S. pombe* cells using a *pho84* probe detected an ~2.3-kb transcript corresponding to the *pho84* mRNA (Fig. 1*B*). By contrast, we did not detect a discrete *prt2* transcript in wildtype cells (Fig. 1*B*). This is consistent with genome-wide RNAseq data (11) showing that the *pho84* transcript is present in log-phase cells, while there are scant sequence reads derived from the SPBC8E4.02c (*prt2*) locus (Fig. S1). However, RNAseq analysis of stationary phase fission yeast cells revealed that the entirety of the *prt2-pho84* locus is transcribed into RNA (Fig. S1). In light of these data, we performed Northern analysis of RNA from stationary phase wildtype *S. pombe* (*lanes WT** in Fig. 1*B*). Now, the *prt2* probe highlighted an ~4.3-kb transcript that was also detected by the *pho84* probe (which also detected the *pho84* mRNA in stationary-phase cells). We surmise that the predominant transcript derived from *prt2* in stationary phase is a *prt2-pho84* read-through lncRNA. (Two minor transcripts of about 1.2 and 1.4 kb were detected in stationary-phase cells by the *prt2* probe but not the *pho84* probe (Fig. 1*B*); these RNAs were not characterized further.)

Further insights were gleaned from Northern analysis of RNA from log-phase *rrp6*Δ cells, in which the *prt2-pho84* read-through lncRNA was present, but the *pho84* mRNA was reduced sharply (Fig. 1*B*).

We employed reverse-transcriptase (RT) primer extension analysis to map the 5′ end of the *prt2* RNA. A ^{32}P-labeled DNA primer complementary to nt −1642 to −1665 upstream of the *pho84* ORF was annealed to total yeast RNA from wildtype or *rrp6*Δ cells and then subjected to reverse transcription. The RT primer extension products were analyzed by denaturing PAGE in parallel with a chain-terminated sequencing ladder generated by DNA polymerase-catalyzed extension of the same ^{32}P-labeled primer annealed to a DNA template extending from nt −1951 to −1482 upstream of the *pho84* ORF (Fig. 1*C*). A predominant 5′ end initiating with adenosine was thereby located 1559 nt upstream of the *pho84* transcription start site (Fig. 1, *A*, *C*, and *D*). A minor 1-nt longer RT primer extension product was also detected (Fig. 1*C*), which signified either (i) transcription initiation at the 5′-flanking T or (ii) an extra RT nucleotide addition opposite a 5′ cap guanosine of the *prt2* RNA. Identical *prt2* RNA ends were detected using a different primer complementary to nt −1597 to −1624 upstream of the *pho84* ORF (not shown). The presence of 10 ATG triplets in the interval between the *prt2* start site and the annotated ATG of the putative SPBC8E4.02c ORF is consistent with *prt2* being a lncRNA rather than an mRNA. In support of this conclusion, deep analyses by mass spectrometry of the protein contents of the fission yeast cell have failed to detect any peptides derived from the putative SPBC8E4.02c ORF (12, 13), while readily detecting the Pho84 polypeptide at a level of ~12,000 molecules per cell (13).

A salient point was that the intensity of the primer extension signal for *prt2* was greater when the analysis was performed with total RNA from *rrp6*Δ cells *versus* wildtype *rrp6*$^+$ cells (Fig. 1*C*, *right panels*; the internal control being that the primer extension signal for actin mRNA was virtually the same when using the equivalent amounts of RNA from *rrp6*Δ and *rrp6*$^+$ cells). By contrast, the primer extension signal for *pho84* mRNA was nearly effaced in *rrp6*Δ cells, suggesting that basal *prt2* and *pho84* expressions are anti-correlated (Fig. 1*C*, *right panels*).

How might we reconcile the observation that the *pho84* mRNA is present by Northern analysis in stationary phase WT cells, but not in log-phase *rrp6*Δ cells, notwithstanding that the *prt2-pho84* read-through transcript was present in both cases. We would speculate that the presence of the *prt2-pho84* read-through RNA in stationary phase reflects an absence of termination of *prt2* transcription prior to reaching the *pho84* poly(A) site that occurs when cells enter into stationary phase. A parsimonious explanation for the presence of *pho84* mRNA in stationary phase cells is that this *pho84* mRNA was synthesized during the period of logarithmic growth that preceded entry

[4] Please note that the JBC is not responsible for the long-term archiving and maintenance of this site or any other third party hosted site.

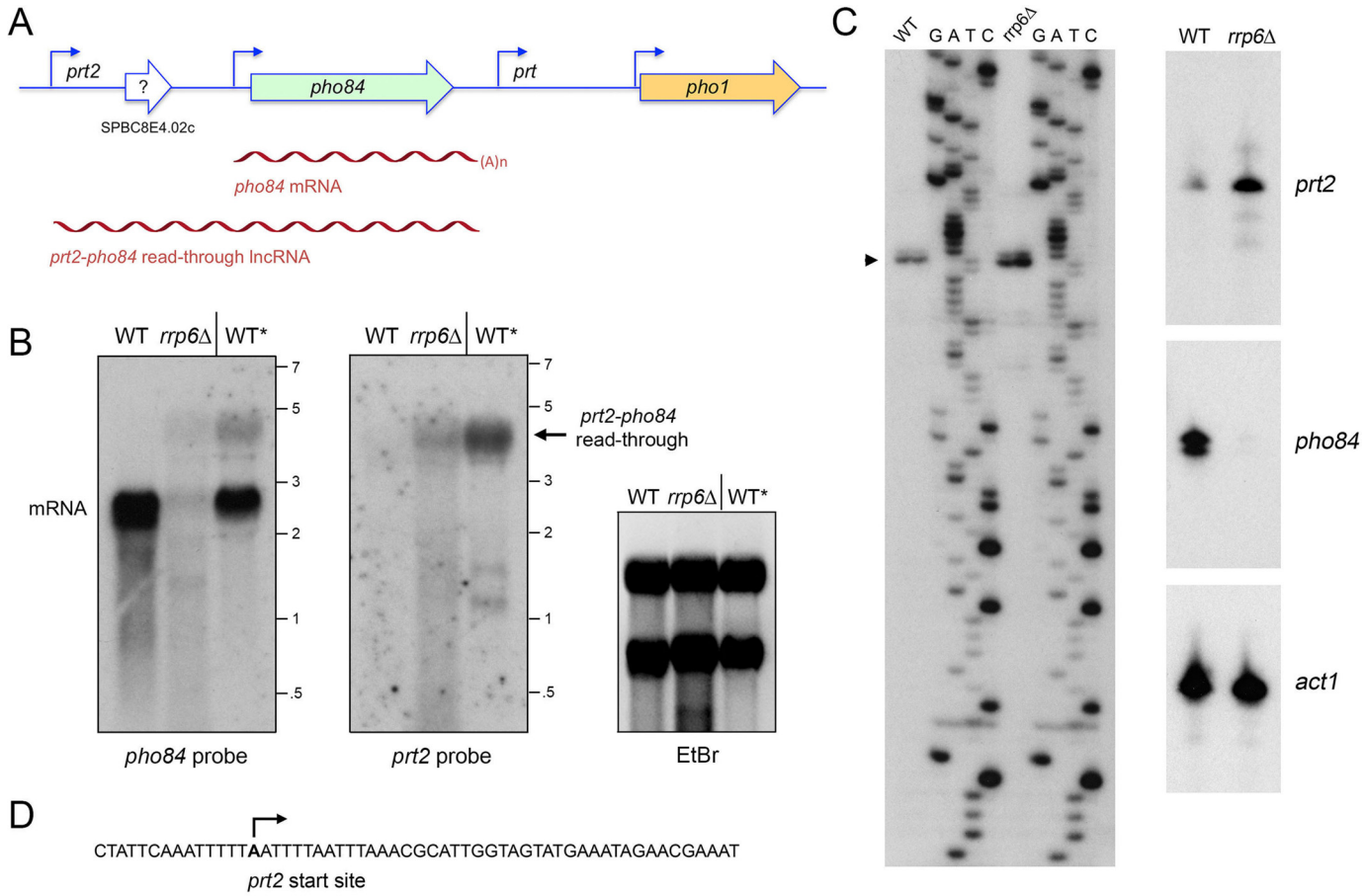

Figure 1. Characterization of a *prt2* lncRNA initiating from the SPBC8E4.02c locus. *A,* schematic illustration of the *S. pombe* chromosome II locus spanning genes SPBC8E4.02c (*prt2*), *pho84*, *prt*, and *pho1*. The *pho84* and *pho1* open reading frames are denoted by *green* and *gold horizontal arrows*, respectively, in the direction of mRNA synthesis. An annotated ORF in the middle of SPBC8E4.02c is depicted as a *blank arrow* with ? indicating the dubiousness of the predicted polypeptide. Experimentally determined 5′ ends of the *pho84* and *pho1* mRNAs and the *prt2* and *prt* lncRNAs are indicated by *bent arrows*. The *pho84* mRNA and *prt2-pho84* read-through lncRNA are depicted as *red wavy lines* below their respective loci. *B,* Northern blot analysis of RNA from exponentially growing wildtype (*WT*) and *rrp6*Δ cells and from stationary phase wildtype cells (*WT**). The RNA was resolved by agarose gel electrophoresis and stained with ethidium bromide to visualize 28S and 18S rRNA (*right panel*) prior to transfer to membrane and hybridization with ^{32}P-labeled *pho84* (*left panel*) or *prt2* (*middle panel*) probes. Annealed probes were visualized by autoradiography. The positions and sizes (kb) of single-stranded RNA markers are indicated on the *right*. *C, left panel,* to map the 5′ end of the *prt2* RNAs, we analyzed the reverse transcriptase primer extension products templated by total RNA from either WT or *rrp6*Δ cells in parallel with a series of DNA-directed primer extension reactions that contained mixtures of standard and chain-terminating nucleotides (the chain terminator is specified *above* the lanes). The primer extension products were analyzed by electrophoresis through a 42-cm denaturing 8% polyacrylamide gel and visualized by autoradiography of the dried gel. The 5′ RNA end is denoted by ▸. *Right panel,* ^{32}P-labeled oligonucleotide primers complementary to *prt2* lncRNA, and *pho84* and *act1* mRNAs were annealed to total RNA from WT or *rrp6*Δ strains and extended with reverse transcriptase. The reaction products were analyzed by denaturing PAGE and visualized by autoradiography. *D,* sense strand DNA sequence flanking the *prt2* transcription start site is shown, with the start site denoted by *bent arrow*.

into stationary phase and that the *pho84* mRNA persists in the cells at the time we harvested them. The situation is different in log-phase *rrp6*Δ cells, as follows. The increased level of *prt2* transcript detected by primer extension likely reflects increased *prt2* stability when the nuclear exosome is defective. Yet, as shown previously for *prt* and *pho1*, it is not simply the steady-state level of the lncRNA that elicits repression of the downstream mRNA, it is the process of lncRNA synthesis across the mRNA promoter that counts. Evidence that the nuclear exosome promotes non-canonical pol II transcription termination in fission yeast (14) has prompted the suggestion that the exosome thereby mitigates read-through RNA synthesis that would interfere with expression of neighboring genes (4, 14–16). In this vein, we envision that an increase in read-through *prt2* transcription in log-phase *rrp6*Δ cells accounts for the observed effacement of *pho84* mRNA.

Insertional inactivation of prt2 de-represses pho84 transcription

We made two versions of a *prt2*-inactivating chromosomal insertion (Fig. 2*A*). The *prt2-Δ1* strain deletes the chromosomal segment from 217 nt upstream of the *prt2* transcription start site to 14 nt downstream of the start site and replaces it with a hygromycin resistance marker (*hygR*) in reverse orientation to *pho84*. Primer extension analysis with a *prt2* antisense primer corresponding to nt +61 to +38 affirmed that the properly initiated *prt2* transcript was present in the wildtype *prt2* strain but absent in *prt2-Δ1* (Fig. 2*B*). The *prt2*-Δ2 strain has the *hygR* marker in lieu of the segment from 217 nt upstream of the *prt2* transcription start site to 532 nt downstream of the start site (Fig. 2*A*). (In this case, no *prt2* primer extension product was detectable, because the sequence to which the antisense primer

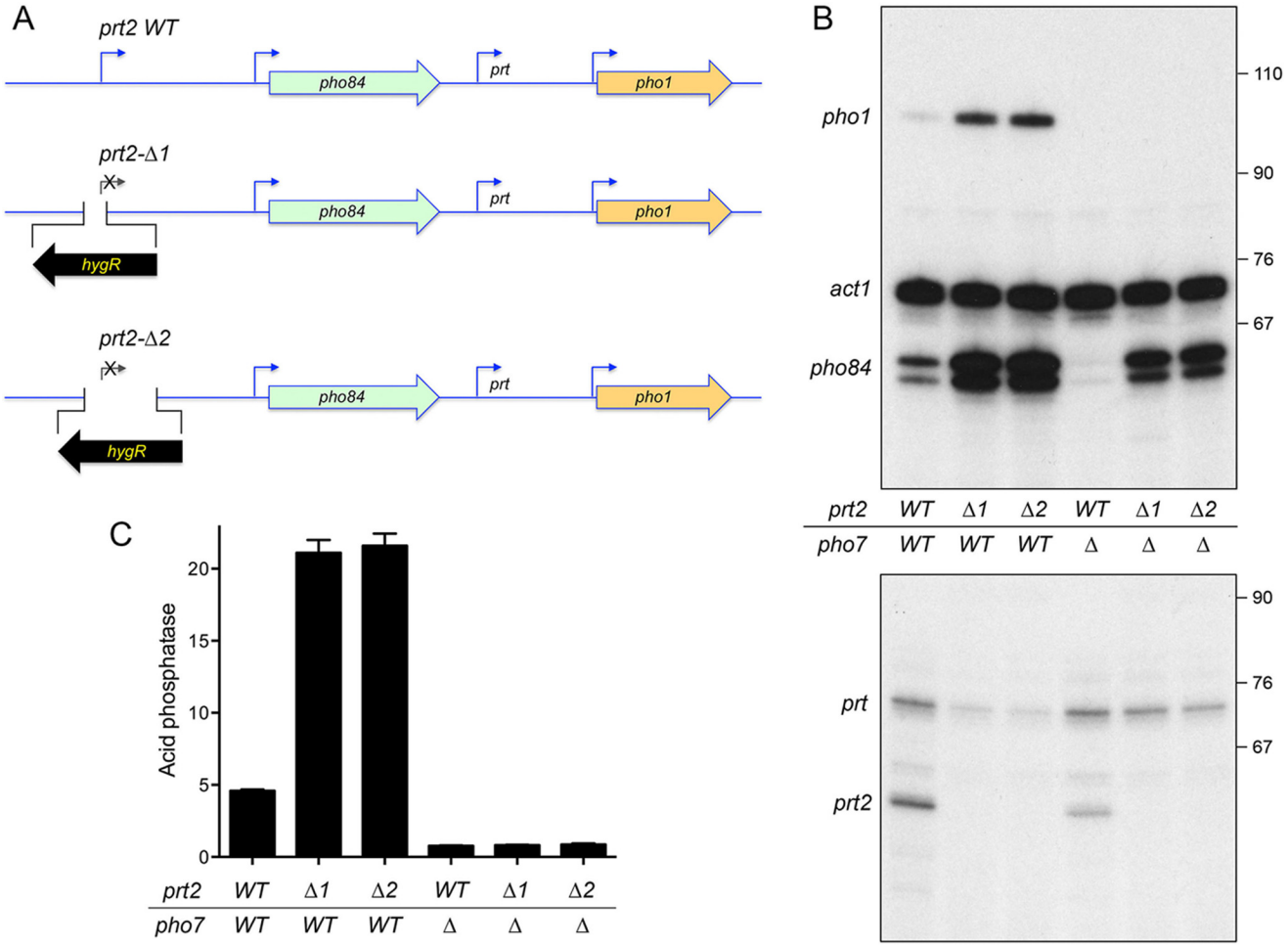

Figure 2. How insertional inactivation of *prt2* affects the expression of downstream genes. *A,* schematic depiction of the wildtype *prt2-pho84-prt-pho1* gene cluster on chromosome II and two *prt2*-inactivating mutants (Δ1 and Δ2) in which the *bracketed* segments flanking the *prt2* transcription start site were deleted and replaced with an oppositely oriented gene that confers hygromycin resistance (*hygR*). *B,* total RNA from fission yeast cells with the indicated *prt2* and *pho7* genotypes was analyzed by reverse transcription primer extension using a mixture of radiolabeled primers complementary to the *pho84*, *act1*, and *pho1* mRNAs (*top panel*) or the *prt* and *prt2* lncRNAs (*bottom panel*). The reaction products were resolved by denaturing PAGE and visualized by autoradiography. The positions and sizes (nt) of DNA markers are indicated on the *right*. *C,* acid phosphatase activity of the indicated strains grown in rich medium was assayed by conversion of *p*-nitrophenyl phosphate to *p*-nitrophenol. The *y* axis specifies the phosphatase activity (A_{410}) normalized to input cells (A_{600}). The *error bars* denote S.E.

anneals was part of the deleted *prt2* DNA.) The instructive findings were that the level of the *pho84* mRNA, as gauged by primer extension, was increased by 3-fold in the *prt2-Δ1* and *prt2-Δ2* strains *versus* the wildtype strain (Fig. 2*B*). Thus, *prt2* transcription down-regulates *pho84* expression and cessation of *prt2* transcription de-represses *pho84* under phosphate-replete conditions.

Cascade effect of prt2 inactivation on downstream prt and pho1 gene expression

Primer extension analysis with a *pho1*-specific antisense primer revealed that insertional inactivation of *prt2* in the *Δ1* or *Δ2* strains elicited a 5-fold increase in the level of *pho1* mRNA compared with wildtype *prt2* (Fig. 2*B*). This induction of *pho1* mRNA expression was also evident at the protein level as a 4-fold increase in cell-surface Pho1 acid phosphatase activity in the *prt2-Δ* strains compared with wildtype (Fig. 2*C*). Primer extension with a *prt*-specific antisense primer showed that *pho1* induction by *prt2-Δ* correlated with a decrease in the level of the repressive upstream *prt* transcript (Fig. 2*B*). These experiments unveiled an unexpected long-range cascade effect of perturbing *prt2-pho84* on the neighboring *prt-pho1* locus. To wit: shutting off *prt2* de-represses *pho84*; increased *pho84* transcription down-regulates *prt*; and reducing *prt* transcription de-represses *pho1*.

Parallel analysis of the wildtype *prt2* and *prt2-Δ* RNA levels in a *pho7Δ* genetic background revealed differential dependences of *pho1* and *pho84* on the Pho7 transcription factor, whereby the induction of *pho1* transcription and acid phosphatase activity via *prt2-Δ* was eliminated in the absence of Pho7 (Fig. 2, *B* and *C*). By contrast, there was substantial residual *pho84* mRNA expression in *pho7Δ prt2-Δ* cells (Fig. 2*B*).

pho84 mRNA polyadenylation sites

To better define the *prt2-pho84-prt-pho1* gene cluster, we mapped the sites of polyadenylation of the *pho84* mRNA by 3′-RACE using as templates total RNA isolated from phosphate-replete and phosphate-starved wildtype cells. Sequencing of 16 independent cDNA clones revealed six different poly(A) sites clustered within a 62-nt segment of the *pho84*

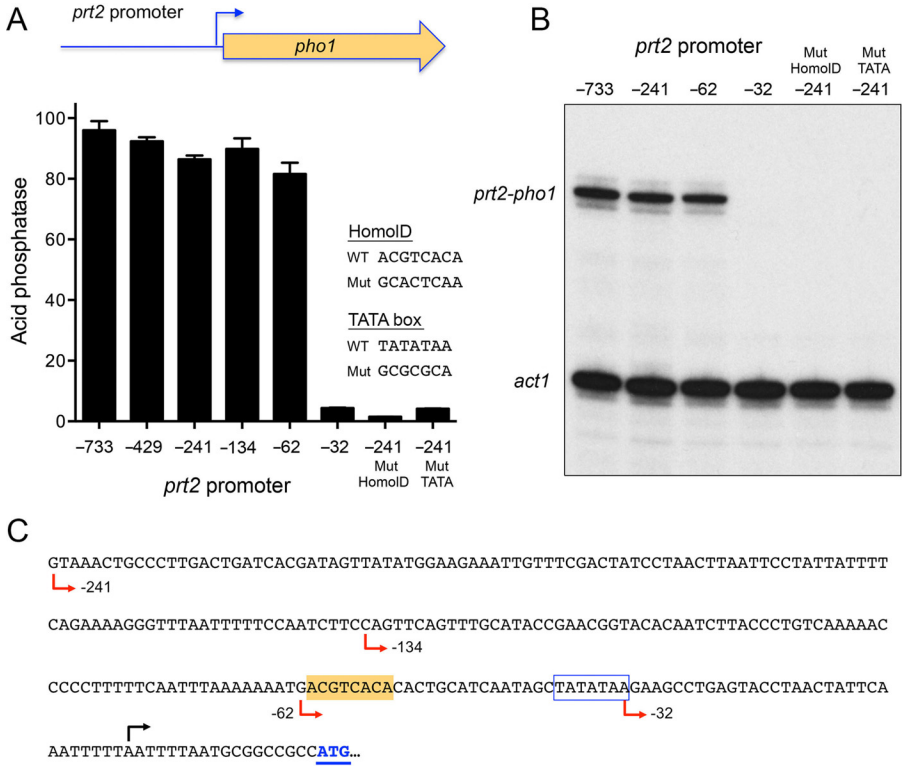

Figure 3. Delineation of the *prt2* promoter. *A,* plasmid reporter of *prt2* promoter activity, wherein the *pho1* ORF was fused to a genomic DNA segment containing nucleotides −733 (or truncated variants as indicated) to +9 of the *prt2* transcription unit. Serial truncations of the upstream margin of the 5′-flanking *prt2* DNA were made at −429, −241, −134, −62, and −32 relative to the *prt2* transcription start site. The indicated mutations in the HomolD-like and TATA box elements were made in the context of the −241 *prt2* promoter. The *prt2-pho1* reporter plasmids were placed into [*prt2-pho84-prt-pho1*]Δ cells. Acid phosphatase activity in phosphate-replete cells was assayed and plotted in *bar graph* format. *B,* primer extension analysis of the *prt2*-driven *pho1* transcript and *act1* mRNA control was performed with total RNA isolated from cells bearing the indicated reporter plasmids. *C,* nucleotide sequence of the *prt2* promoter reporter is shown from positions −241 to the ATG start codon of the *pho1* ORF. The *pho1* ATG start codon is in *blue* and *underlined*. The *prt2* transcription start site is indicated by *black arrow* above the DNA sequence. Margins of promoter truncations are indicated by *red arrows below* the DNA sequence. A putative TATA element is outlined by a *blue box*. A putative HomolD-like element is *shaded gold*.

3′UTR. 6/16 cDNA clones had the identical junction to a poly(A) tail at a site 230 nt downstream of the *pho84* translation stop codon (Fig. S2). 4/16 cDNA clones had a poly(A) site 234 nt downstream of the *pho84* stop codon. These two predominant *pho84* poly(A) sites are located 16 and 20 nt downstream of a fission yeast AAUAAA polyadenylation signal (PAS) (Fig. S2) (17). In addition, two cDNA clones had poly(A) sites 13 nt downstream of this PAS, and one cDNA clone was polyadenylated 30 nt downstream of this PAS. The remaining three cDNA clones defined two other poly(A) sites 183 and 185 nt downstream of the *pho84* stop codon (Fig. S2). These poly(A) sites are located 18 and 20 nt downstream of a separate AAUAAA polyadenylation signal (Fig. S2). The major *pho84* poly(A) site is 158 nt upstream of the transcription start site of the flanking *prt* lncRNA and 83 nt upstream of the HomolD box of the *prt* promoter. pol II elongation complexes synthesizing the *pho84* mRNA will undergo nascent strand 3′ cleavage at the poly(A) sites and (in all likelihood) ensuing transcription termination (18) within the downstream DNA region that overlaps the *prt* promoter, thereby suggesting a scenario for how increased *pho84* transcription could interfere with *prt* transcription.

prt2 transcription: What comprises a prt2 promoter?

To address this question, we constructed a plasmid reporter in which the *pho1* ORF and its native 3′-flanking DNA was fused immediately downstream of a genomic DNA segment containing nt −733 to +9 of the *prt2* transcription unit (Fig. 3*A*). Because this plasmid generated vigorous acid phosphatase activity when introduced into a strain that was deleted for the entire *prt2-pho84-prt-pho1* gene cluster (Fig. 3*A*), we surmised that the 733-nt segment embraces a *prt2* promoter. To demarcate *cis*-acting elements, we serially truncated the 5′-flanking DNA to positions −429, −241, −134, −62, and −32 upstream of the *prt2* transcription start site. The acid phosphatase activity of the plasmid-bearing [*prt2-pho84-prt-pho1*]Δ cells indicated that the 5′-flanking 62-nt segment sufficed for *prt2* promoter-driven expression (Fig. 3*A*). Further truncation to −32 effaced acid phosphatase activity (Fig. 3*A*). Primer extension analysis using a *pho1* antisense primer revealed correct initiation at the *prt2* start site in the plasmid reporter and virtually equivalent levels of the *prt2*-driven *pho1* mRNA from the −733, −241, and −62 promoters, but no detectable *prt2*-driven *pho1* RNA from the −32 reporter strain (Fig. 3*B*).

HomolD-like and TATA boxes are essential for prt2 promoter activity

The 241-nt DNA segment flanking the *prt2* start site is shown in Fig. 3*C*. The promoter deletion analysis suggested the presence of essential transcriptional elements between −62 and −32. Our inspection of this segment disclosed a potential

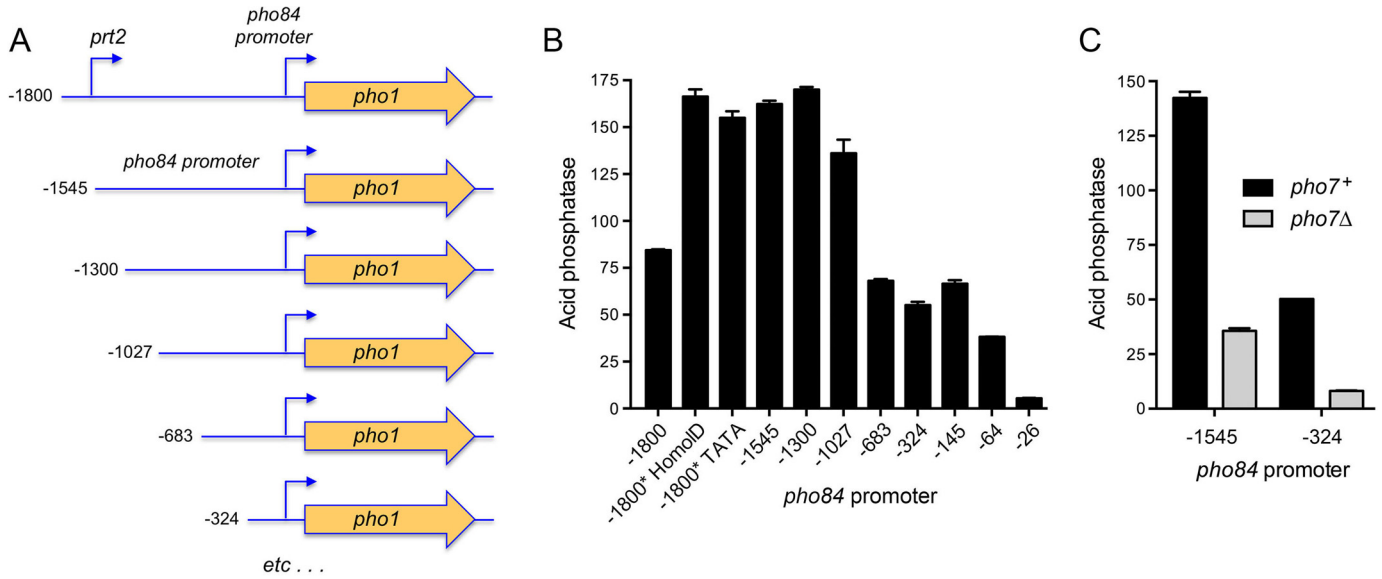

Figure 4. Demarcation of the *pho84* promoter. *A,* plasmid reporters of *pho84* promoter, in which the *pho1* ORF was fused to a genomic DNA segment containing nucleotides −1800 (or truncated variants as indicated) to +151 of the *pho84* transcription unit. The −1800 construct includes the *prt2* promoter; *prt2* HomolD and TATA box mutations (as per Fig. 3) were made in the context of the −1800 *pho84·pho1* reporter plasmid. *B,* acid phosphatase activity of [*prt2-pho84-prt-pho1*]Δ cells bearing the indicated *pho84* promoter reporter plasmids. *C,* acid phosphatase activity of *pho7*$^{+}$ and *pho7*Δ cells bearing the −1545 or −324 *pho84* promoter reporters.

HomolD-like box (*shaded yellow* in Fig. 3*C*). The consensus HomolD element 5′-CAGTCAC(A/G) functions as a pol II promoter signal in fission yeast genes encoding ribosomal proteins (19–21) and in the *prt* and *nc-tgp1* lncRNA genes that control phosphate homeostasis (6, 8). The *prt2* HomolD-like sequence ($^{-61}$ACGTCACA^{-54}) deviates by two nucleobases from the consensus. The *prt2* promoter also contains a TATA box sequence $^{-38}$TATATAA^{-32}. To query the role of the HomolD and TATA elements in *prt2* function, we introduced a HomolD mutant (GCACTCAA) or a TATA mutant (GCGCGCA) into the −241 *prt2·pho1* reporter. Both mutations effaced acid phosphatase activity (Fig. 3*A*) and expression of the *prt2·pho1* reporter RNA (Fig. 3*B*). Thus, the *prt2* lncRNA promoter shares the bi-partite HomolD/TATA architecture of the *prt* and *nc-tgp1* lncRNA genes.

Plasmid-based reporter to study expression of pho84

As depicted in Fig. 4*A*, we isolated a fragment of the *prt2-pho84* locus, spanning from 1800 nt upstream of the *pho84* transcription initiation site (and encompassing the *prt2* promoter) to 151 nt downstream of the *pho84* transcription start site (representing the complete 5′-UTR of the *pho84* mRNA) and fused it to the *pho1* ORF and its native 3′-flanking DNA. To gauge the impact of upstream *prt2* activity on the downstream *pho84* promoter, we introduced the *prt2* promoter-inactivating HomolD and TATA box mutations into the −1800 *prt2-pho84·pho1* reporter. We also deleted the *prt2* promoter by truncating the upstream margin to −1545 relative to the *pho84* transcription start site (Fig. 4*A*). The reporter plasmids were introduced into [*prt2-pho84-prt-pho1*]Δ cells, and Pho1 acid phosphatase activity was measured under phosphate-replete conditions. The basal level of Pho1 expression from the −1800 reporter was increased 2-fold by deletion of the *prt2* promoter (as in the −1545 construct) or by mutations of the HomolD or TATA boxes in the context of the −1800 reporter (Fig. 4*B*). We surmise that the *prt2-pho84·pho1* reporter recapitulates *prt2* lncRNA repression of transcription from the *pho84* promoter.

To further define the *pho84* promoter, we serially truncated the 5′ margins of the *pho84·pho1* reporter constructs to positions −1300, −1027, −683, −324, −145, −64, and −26 upstream of the *pho84* transcription start site (Fig. 4*A*). High Pho1 activity was maintained for the −1545, −1300, and −1027 promoters, followed by a step down to intermediate Pho1 activity for the −683, −324, and −145 promoters (*i.e.* activity of the −683 and −145 reporters was 41% of the −1545 construct) (Fig. 4*B*). Truncations to −64 and −26 reduced Pho1 expression to 23 and 3% of the −1545 reporter, respectively. The essential segment between −64 and −26 includes a TATA box ($^{-33}$TATATATA^{-26}).

In light of the RNA analyses suggesting that *pho84* expression is incompletely reliant on Pho7 (Fig. 2*B*), we compared Pho1 activity driven by the −1545 and −324 *pho84* promoters in *pho7*$^{+}$ and *pho7*Δ strain backgrounds. Absent Pho7, the −1545 and −324 promoters were 25 and 16% as active as in the presence of Pho7 (Fig. 4*C*). The residual Pho7-independent activity of the *pho84* promoter echoes that of the *tgp1* promoter, *i.e.* acid phosphatase activity driven by the *tgp1* promoter was reduced by 85% in a *pho7*Δ strain background (10).

Pho7-binding sites in the pho84 promoter

To locate Pho7 site(s), a series of overlapping ^{32}P-labeled DNA fragments spanning the genomic region from nt −1300 to +151 relative to the *pho84* transcription start site was prepared and tested by EMSA for binding to purified recombinant Pho7-DBD (DNA-binding domain; amino acids 279–368) (10). Whereas there was no protein-DNA complex formed on a DNA fragment spanning from −1300 to −1028, the DNA fragment from −1102 to −816 was bound by Pho7-DBD to form a single protein–DNA complex of slower electrophoretic mobility (Fig. 5). Pho7-DBD also formed a single protein–DNA com-

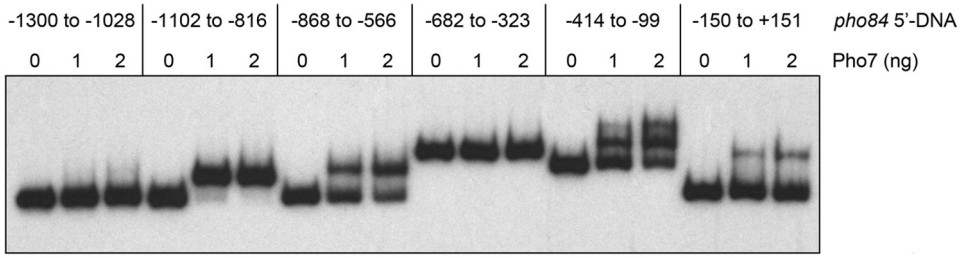

Figure 5. Pho7-binding sites in the *pho84* promoter. EMSAs using ^{32}P-labeled DNA fragments embracing the indicated sequences upstream of the *pho84* transcription start site (defined as +1). The nucleotide margins of the DNA segments are indicated at the *top*. Reaction mixtures (10 μl) containing 0.05 pmol of labeled DNA, 340 ng of poly(dI-dC), and 0–2 ng of Pho7-DBD were incubated for 10 min at room temperature. The mixtures were analyzed by native PAGE. An autoradiograph of the gel is shown.

plex on DNA fragments from −868 to −566 and −150 to +151, albeit with lower affinity than for the −1102 to −816 fragment, as gauged by the amount of shifted complex formed as a function of input Pho7-DBD (Fig. 5). The DNA segment from −414 to −99 formed two sequentially shifted complexes with Pho7-DBD, again with lower apparent affinity than the −1102 to −816 fragment (Fig. 5).

To map the high-affinity site within the −1102 to −816 segment, we conducted DNase I footprinting experiments. Initial tests using the entire 287-nt fragment located a single region of protection from DNase I between approximately −995 and −962 (data not shown). To better resolve the footprint margins, we exploited a shorter DNA probe, from nt −1039 to −907, that was 5′ ^{32}P-labeled on the top strand or the bottom strand. A single region of protection from DNase I cleavage spanned nt −988 to −971 on the top strand (Fig. 6*A*) and nt −974 to −991 on the bottom strand (Fig. 6*B*). The footprint is denoted by brackets over the DNA sequence in Fig. 6*C*, and it embraces a 12-mer sequence 5′-($^{-977}$TCGGTCTTTGAA^{-988}) (on the bottom strand) that is identical at 8/12 positions to Pho7-binding "site 2" in the *pho1* promoter (5′-TCGGAAATTAAA) and at 9/12 positions to the Pho7-binding "site 1" in the *pho1* promoter (5′-TCGCTGCTTGAA). It is worth noting that the Pho7-binding motif that we define here in the *pho84* promoter is on the bottom DNA strand and oriented away from the *pho84* transcription unit, whereas the two Pho7 sites in the *pho1* promoter are spaced closely on the top DNA strand and oriented toward the *pho1* transcription unit (10).

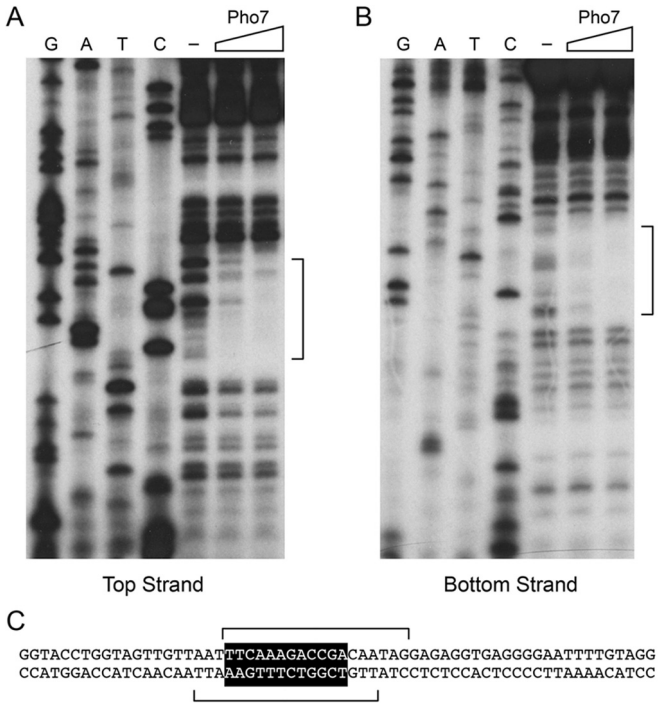

Figure 6. Footprinting of a high-affinity Pho7 site in the *pho84* promoter. DNase I footprinting analyses of the top strand (*A*) and bottom strand (*B*) of the *pho84* promoter fragment from −1039 to −907 nt upstream of the transcription start site are shown along with the respective sequencing ladders. Binding reaction mixtures contained 0.25 pmol of 5′ ^{32}P-labeled DNA and either no added Pho7-DBD (*lanes* −) or increasing amounts of Pho7-DBD (5 or 10 ng). The margins of the footprints are indicated by *brackets*. DNA sequence from −1008 to −947 upstream of the *pho84* transcription start site is shown in *C*. The Pho7-binding motif is shown in *white font on black background*. The *brackets* denote the DNase I footprints on the top and bottom strands.

Effect of CTD phospho-site mutations on prt2 regulated pho84 expression

Previous studies had shown that repression of *pho1* expression from the *prt-pho1* locus (in either chromosomal or plasmid contexts) in phosphate-replete cells is affected by pol II CTD phosphorylation status, as gauged by the impact of CTD mutations that eliminate particular phosphorylation marks (5, 6, 22). For example, the inability to place a Ser7-PO_4 mark in *S7A* cells de-repressed *pho1*. Limiting the number of serine 5 CTD sites to three consecutive Ser5-containing CTD heptads also de-repressed *pho1*. By contrast, the inability to place a Thr4-PO_4 mark in *T4A* cells hyper-repressed *pho1* under phosphate-replete conditions. Here, to test the impact of these CTD mutations on *prt2*-regulated *pho84* promoter-driven gene expression, we introduced a −2292 *prt2-pho84·pho1* reporter plasmid (Fig. 7*A*) into [*prt2-pho84-prt-pho1*]Δ cells in which the *rpb1* chromosomal locus was replaced by alleles *rpb1-CTD-WT*, *-CTD-T4A*, *-CTD-S7A*, *-CTD-T4A·S7A*, or *-CTD-$S5_3S5A_{11}$* (23, 24). Whereas the *T4A* allele hyper-repressed Pho1 expression by 4-fold in phosphate-replete cells, the *S7A* and *$S5_3S5A_{11}$* CTD variants elicited 2- and 3-fold increases in activity compared with the *rpb1-CTD-WT* (Fig. 7*A*). The de-repression of the *prt2-pho84·pho1* reporter by *S7A* was eliminated in a *rpb1-CTD-T4A·S7A* strain in which acid phosphatase activity was instead hyper-repressed, thereby phenocopying the *T4A* single mutant (Fig. 7*A*).

prt2 and pho84 promoter activities are not affected by pol II CTD mutations

To query whether CTD mutations influence *prt2* promoter-driven transcription, we introduced the −241 *prt2·pho1*

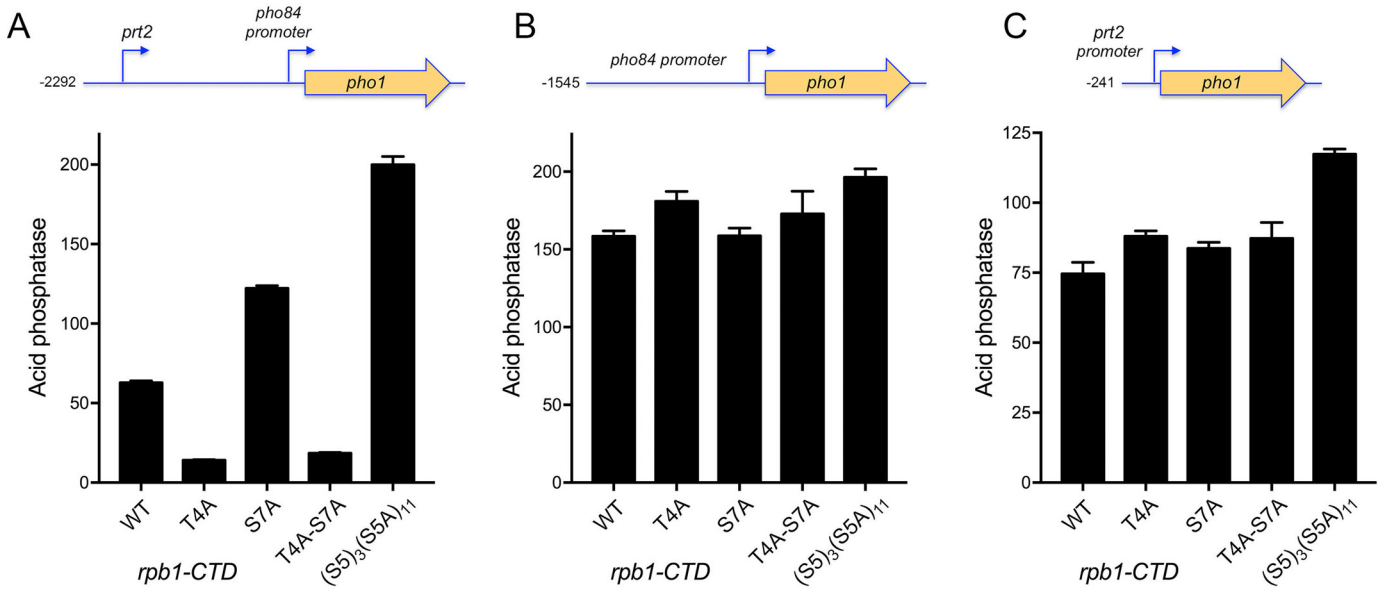

Figure 7. Effect of CTD phospho-site mutations on *prt2*-regulated *pho84* expression and individual *prt2* and *pho84* promoter activities. [*prt2-pho84-prt-pho1*]Δ *rpb1-CTD* strains with wildtype or mutated heptad arrays as specified were transformed with reporter plasmids *prt2-pho84·pho1* (*A*), *pho84·pho1* (*B*), or *prt2·pho1* (*C*) and assayed for acid phosphatase activity.

reporter plasmid into the [*prt2-pho84-prt-pho1*]Δ *rpb1-CTD* strains and measured acid phosphatase expression (Fig. 7*C*). *prt2*-promoted Pho1 activity was similar in the *WT*, *T4A*, *S7A*, and *T4A·S7A* strains and was 50% higher in the $S5_3S5A_{11}$ strain. From these results, we conclude the following: (i) the de-repression of the *prt2-pho84·pho1* reporter in *S7A* and $S5_3S5A_{11}$ cells (Fig. 7*A*) was not caused by a decrease in transcription from the *prt2* lncRNA promoter; and (ii) hyper-repression of the *prt2-pho84·pho1* reporter in *T4A* and *T4A·S7A* cells (Fig. 7*A*) was not caused by an increase in transcription from the *prt2* lncRNA promoter.

To interrogate the *pho84* promoter, we placed the −1545 *pho84·pho1* reporter plasmid in the [*prt2-pho84-prt-pho1*]Δ *rpb1-CTD* strains and measured acid phosphatase activity (Fig. 7*B*), which was similar in the *WT*, *T4A*, *S7A*, *T4A·S7A*, and $S5_3S5A_{11}$ backgrounds. Thus, the de-repression or hyper-repression of the *prt2-pho84·pho1* reporter by the CTD phospho-site mutant is not reflective of increased or decreased activity of the *pho84* promoter *per se*.

Fleshing out the cascade model for prt2 action at a distance on the pho1 promoter

The cascade effect of perturbing *prt2* on the downstream *pho84*, *prt*, and *pho1* transcription units suggested by the *prt2*-Δ experiments (Fig. 2) is amenable to further testing in light of the implementation of reporter assays and initial functional mapping of the *prt2* and *pho84* promoters. For example, having defined a mutation of the *prt2* TATA box that eliminates *prt2* transcription (Fig. 3), we introduced the *prt2* TATA mutation into a *prt2-pho84-prt-pho1* reporter plasmid that contains the complete 4-gene phosphate regulon (Fig. 8*C*), thereby allowing us to gauge *prt2* long-range action on *pho1* expression via assay of acid phosphatase activity. We found that the *prt2* TATA mutation elicited a 2-fold increase in *pho1* expression (Fig. 8*C*). Whereas this effect of *prt2* TATA mutation on the *pho1* gene correlated nicely with the 2-fold increase it exerts on the activity of the *pho84* promoter (Fig. 4*B*), we thought it important to test whether intervening *pho84* transcription is essential for *prt2-TATA*'s effect on *pho1*. To do so, we needed to interdict *pho84* transcription by inactivating its promoter. This was achieved by mutating the *pho84* TATA box element $^{-33}$TATATATA^{-26} to CGCGCGCG (Fig. 8*A*). The *pho84* TATA mutation in the context of the −1545 *pho84·pho1* reporter reduced *pho84* promoter activity to 4% of the wildtype control (Fig. 8*A*). The salient finding was that the *pho84* TATA mutation in the context of the *prt2-pho84-prt-pho1* locus blocked the de-repression of *pho1* expression elicited by the *prt2* TATA mutation (Fig. 8*C*), thereby showing that *pho84* transcription is necessary for the cascade effect.

A key missing link in the model is to establish whether *pho84* transcription influences the activity of the flanking *prt* promoter. To address this issue, we employed a reporter in which the genomic DNA segment spanning the *pho84* gene and the *prt* promoter was fused to the *pho1* ORF (Fig. 8*B*). Into this construct, we introduced the *pho84* TATA mutation. The instructive finding was that the *prt* promoter-driven acid phosphatase activity was increased 4-fold by the *pho84* TATA mutation. This result affirms that *pho84* transcription interferes with the downstream flanking *prt* promoter.

Discussion

Fission yeast phosphate homeostasis entails repressing the *pho84*, *pho1*, and *tgp1* genes during phosphate-replete growth and inducing/de-repressing them under conditions of phosphate starvation. This study extends and consolidates a shared basis for repression of all three genes of the phosphate regulon, in which transcription of lncRNAs from the upstream *prt2*, *prt*, and *nc-tgp1* genes interferes with the downstream *pho84*, *pho1*, and *tgp1* promoters. The simplest model for interference is that pol II synthesizing the lncRNA displaces transcription factor

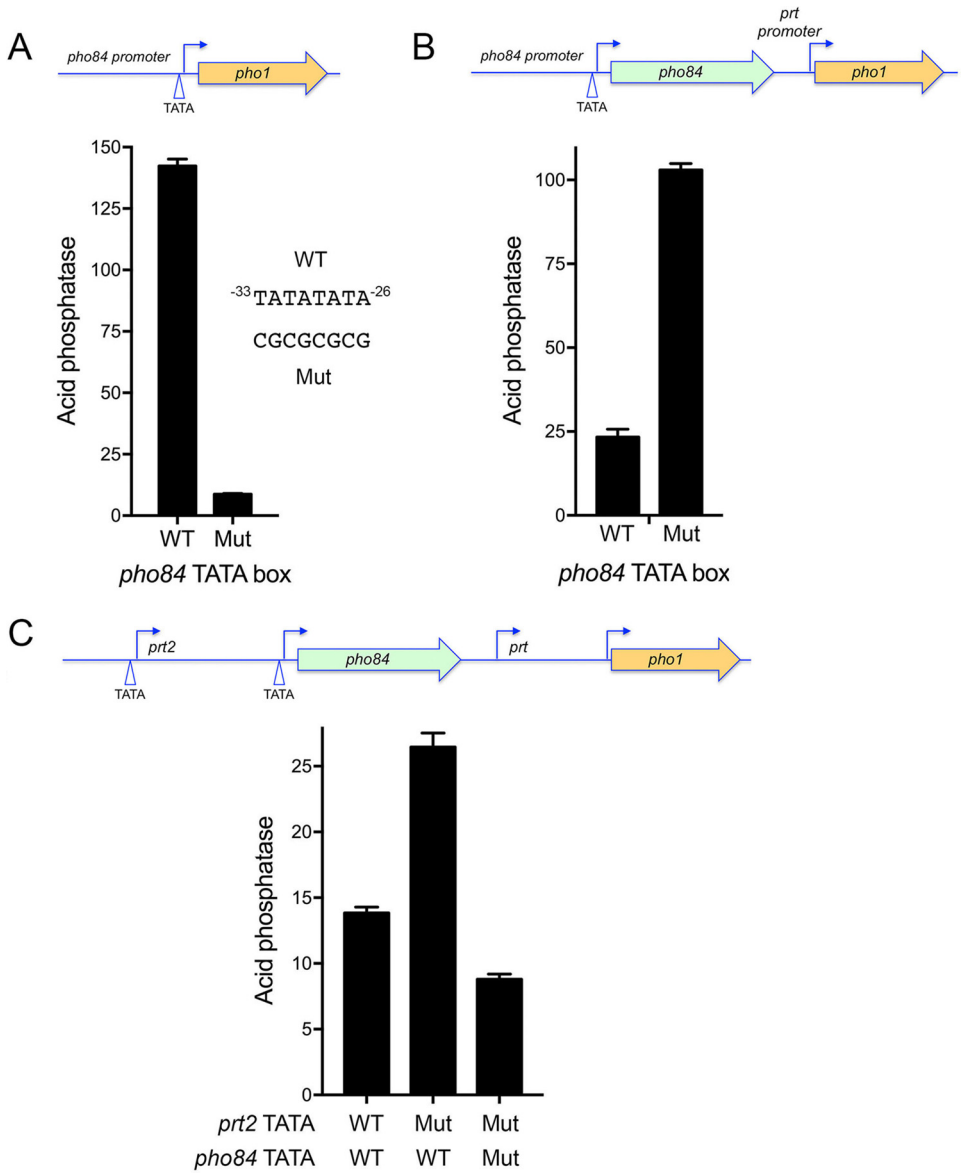

Figure 8. Testing a cascade model for *prt2* action at a distance on the *pho1* promoter. *A,* acid phosphatase activity expressed from a *pho84*·*pho1* reporter in which the *pho84* TATA box was either wildtype (*WT*) or mutated (*Mut*) as indicated. *B,* acid phosphatase activity expressed from a *pho84-prt*·*pho1* reporter in which the *pho84* TATA box was either wildtype or mutated. *C,* acid phosphatase activity expressed from a *prt2-pho84-prt-pho1* reporter in which the *prt2* and *pho84* TATA boxes were either wildtype or mutated as specified.

Pho7 from its binding sites in the *pho1*, *pho84*, and *tgp1* promoters that overlap the lncRNA transcription unit. In the case of *nc-tgp1* repression of *tgp1*, the cleavage/poly(A) site of the *nc-tgp1* lncRNA (5′-UCGGA ↓) is located 187 nt upstream of the *tgp1* transcription start site, exactly within the Pho7 DNA-binding site of the *tgp1* promoter (5′-TCGGA ↓ CATTCAA) (8). The situation is different for *prt2* and *prt* lncRNAs, for which the predominant species detected are a *prt2-pho84* read-through RNA (Fig. 1) and a *prt-pho1* read-through RNA (3, 4), respectively.

Here, we show that the bi-partite HomolD/TATA-box architecture described previously for the *prt* and *nc-tgp1* promoters (6, 8) is also applicable to the *prt2* promoter. We envision that this distinctive promoter arrangement somehow couples lncRNA transcription to phosphate availability, whereby the *prt2*, *prt*, and *nc-tgp1* promoters are active in phosphate-replete cells and turned off in response to phosphate starvation. The mechanism of HomolD-dependent pol II transcription and its regulation are largely uncharted. Inositol polyphosphate IP_7 is a signaling molecule that controls the level of *pho1* and *pho84* expression in phosphate-replete cells, such that IP_7 phosphatase mutants unable to degrade IP_7 are de-repressed and IP_6 kinase mutants unable to synthesize IP_7 are hyper-repressed (9, 25). Whether and how IP_7 affects the synthesis of the phosphate-regulatory lncRNAs are unknown.

Our studies here of the effects of pol II CTD phospho-site mutations on *prt2*-responsive *pho84* transcription echo previous findings for *prt-pho1* and *nc-tgp1-tgp1*, *viz.* the *pho84* promoter in the tandem *prt2-pho84* array is de-repressed by *S7A* and $S5_3S5A_{11}$, implicating the Ser5-PO_4 and Ser7-PO_4 marks as important for enforcement of the repressive status. The de-repressive CTD mutations do not affect the activity of the *prt2*

lncRNA or *pho84* mRNA promoters *per se*, suggesting that they exert their effects via an increased propensity to terminate lncRNA synthesis prior to the Pho7 sites in the *pho84* promoter, as invoked initially for *prt-pho1* (6). As with *prt-pho1*, we see that CTD *T4A* mutation hyper-represses the *pho84* promoter in the tandem *prt2-pho84* array (conceivably by decreasing the lncRNA transcription termination) and that hyper-repression is maintained in a *T4A/S7A* double mutant. It is worth noting that *S7A* and *T4A* exert similar up and down effects on the PHO regulon in phosphate-replete cells as do the IP_7 phosphatase and IP_6 kinase mutants, raising the speculation that CTD-dependent transactions might be a target of IP_7 signaling.

The tightly clustered arrangement of the *prt2*, *pho84*, *prt*, and *pho1* transcription units in the fission yeast genome is intriguing, insofar as lncRNA genes alternate with mRNA genes in service of the same biological response pathway. Whereas studies here and previously show that the *prt-pho1* and *prt2-pho84* gene pairs are "autonomous" in their suppression of downstream mRNA synthesis by upstream lncRNA transcription under phosphate-replete conditions and their induction of mRNA synthesis during phosphate starvation, the experiments here highlight an unexpected (at least to us) facet of the four-gene cluster arrangement, whereby permutation of *prt2* expression exerts a cascade effect on the downstream *prt* and *pho1* loci. Specifically, the inactivation of *prt2* lncRNA transcription, via deletion or mutation of the *prt2* promoter (in the native chromosomal locus or on a reporter plasmid), elicits up-regulation of both *pho84* and *pho1*. The interesting new wrinkle to this cascade effect is that transcription of an upstream mRNA gene (*pho84*) represses the expression of a downstream flanking lncRNA gene (*prt*), which is, in effect, a role reversal for mRNA transcription as the agent of repression by transcriptional interference rather than the target of such transcriptional interference.

Experimental procedures

Insertional inactivation of prt2

We constructed two *prt2*Δ cassettes, Δ1 and Δ2. The 5′- and 3′-flanking homology arms were cloned upstream and downstream of a hygromycin resistance gene (*hygMX*) in the pMJ696 vector. The 5′ homology flank of both cassettes extended from nt −733 to −218 upstream of the *prt2* transcription start site. The 3′ homology arm of *prt2*Δ-1 extended from nt +15 to +532 downstream of the *prt2* transcription start site. The 3′ homology arm of *prt2*Δ-2 extended from nt +533 to +1083. The *prt2*Δ-1 and *prt2*Δ-2 knock-out cassettes were excised from the plasmid and transformed into wildtype *S. pombe* diploids. Hygromycin-resistant diploids were checked by Southern blot analysis for a correct insertion-deletion event and subsequently sporulated on Malt plates to obtain hygromycin-resistant haploid *prt2*Δ-1 and *prt2*Δ-2 strains.

Deletion of the prt2-pho84-prt-pho1 gene cluster

The deletion of the entire *prt2-pho84-prt-pho1* four-gene locus was constructed by cloning 5′ *prt2*-flanking and 3′ *pho1*-flanking homology arms upstream and downstream of *hygMX* in the pMJ696 vector. The 5′ homology flank extended from −733 to −218 nucleotides upstream of the *prt2* transcription start site. The 3′ homology flank extended from nt +1336 to +2009 downstream of the *pho1* start codon. The [*prt2-pho84-prt-pho1*]Δ cassette was excised from the plasmid and transformed into wildtype *S. pombe* diploids. Correct replacement of the *prt2-pho84-prt-pho1* locus by the hygromycin-resistance marker was confirmed by Southern blot analysis, and the heterozygous diploid was sporulated to obtain hygromycin-resistant [*prt2-pho84-prt-pho1*]Δ haploids.

Reporter plasmids

We constructed five sets of *pho1*-based reporter plasmids, marked with a kanamycin-resistance gene (*kanMX*), in which the expression of Pho1 acid phosphatase was driven by either (i) a *prt2*(promoter) element (Fig. 3); (ii) a *pho84*(promoter) element (Fig. 4); (iii) a tandem *prt2*(promoter + lncRNA)–*pho84*(promoter) element (Fig. 4*A*); (iv) a tandem *pho84* (promoter + mRNA)–*prt*(promoter) element (Fig. 8*B*); or (v) a native *prt2-pho84-prt-pho1* gene array (Fig. 8*C*). Plasmids i–iv are derivatives of p*KAN*-(*pho1*) described previously (6) that were generated by insertion of various genomic sequences flanking *pho1*, as specified under "Results" and figure legends. Serial truncations from the 5′ ends of the *prt2* and *pho84* promoters were made at the margins depicted in the figures. Nucleotide substitutions in HomolD or TATA promoter elements were made as depicted in the figures. The inserts of all plasmids were sequenced to exclude unwanted mutations.

Reporter assays

Reporter plasmids were transfected into [*prt2-pho84-prt-pho1*]Δ cells. *kanMX* transformants were selected on YES (yeast extract with supplements) agar medium containing 150 μg/ml G418. Single colonies of transformants (≥20) were pooled and grown at 30 °C in plasmid-selective liquid medium. To quantify acid phosphatase activity, reaction mixtures (200 μl) containing 100 mM sodium acetate, pH 4.2, 10 mM *p*-nitrophenyl phosphate, and cells (ranging from 0.005 to 0.1 A_{600} units) were incubated for 5 min at 30 °C. The reactions were quenched by adding 1 ml of 1 M sodium carbonate; the cells were removed by centrifugation, and the absorbance of the supernatant was measured at 410 nm. Acid phosphatase activity is expressed as the ratio of A_{410} (*p*-nitrophenol production) to A_{600} (cells). Each datum in the graphs is the average (±S.E.) of phosphatase assays using cells from at least three independent cultures.

RNA analyses

Total RNA was extracted via the hot phenol method from 15 A_{600} units of yeast cells that had been grown to mid log-phase (A_{600} of 0.3 to 0.8) at 30 °C in YES or YES + G418 (for selection of *kanMX* plasmids). RNA was also isolated from stationary phase cells grown in YES medium at 30 °C to A_{600} of 3.7. The RNAs were extracted serially with phenol/chloroform and chloroform, and then precipitated with ethanol. The RNAs were resuspended in 10 mM Tris-HCl, pH 6.8, 1 mM EDTA. For Northern blotting, equivalent amounts (15 μg) of total RNA were resolved by electrophoresis through a 1.2% agarose/formaldehyde gel. After photography under UV illumination to visu-

alize ethidium bromide-stained 18S and 28S rRNAs, the gel contents were transferred to an Amersham Biosciences Hybond-XL membrane (GE Healthcare). [^{32}P]dAMP-labeled hybridization probes were prepared by random-priming radiolabeling of DNA fragments of the *pho84* gene (spanning nucleotides +916 to +1840 relative to *pho84* transcription start site) or the *prt2* gene (spanning nucleotides −1545 to −99 relative to *pho84* transcription start site). Hybridization was performed as described (26), and the hybridized probes were visualized by autoradiography.

Aliquots (10 or 20 μg) of total RNA were used as templates for Moloney murine leukemia virus reverse transcriptase-catalyzed extension of 5′ ^{32}P-labeled oligodeoxynucleotide primers complementary to the *pho84*, *pho1*, or *act1* mRNAs and the *prt2* or *prt* lncRNAs. The primer extension reactions were performed as described previously (27), and the products were analyzed by electrophoresis of the reaction mixtures through a 22-cm 8% polyacrylamide gel containing 7 M urea in 80 mM Tris borate, 1.2 mM EDTA. The ^{32}P-labeled primer extension products were visualized by autoradiography of the dried gel. The primer sequences were as follows: *act1* 5′-GATTTCTTCTTCCATGGTCTTGTC; *pho1* 5′-GTTGGCACAAACGACGGCC; *pho84* 5′-AATGAAGTCCGAATGCGGTTGC; *prt2* 5′-TCTCATCCTCTATGACTTATTTCG; and *prt* 5′-TTTGCATGCCTAGTTTTCCTTGAC. The primer for detection of the *prt2* promoter-driven *pho1* mRNA (in Fig. 3*B*) was 5′-GGAAGTCAAATGTTCCTTG.

To precisely map the 5′ end of the *prt2* RNA, we used a ^{32}P-labeled primer complementary to *prt2* (5′-TAATTCTATCTCATCCTCTATGAC) for RT primer extension templated by total RNA isolated from wildtype or *rrp6*Δ cells. The RT products were then analyzed by electrophoresis through a 42-cm denaturing 8% polyacrylamide gel in parallel with a series of DNA-directed primer extension reactions (using the same labeled *prt2* primer) that contained mixtures of standard and chain-terminating nucleotides, as described (17).

3′-RACE

To map the poly(A) site of the *pho84* mRNA, we employed the 3′-RACE kit (Invitrogen). Total RNA was isolated from phosphate-replete cells and from cells harvested 6 h after transfer to phosphate-free medium. 2 μg of RNA was used as template for first strand cDNA synthesis by SuperScript II RT and an oligo(dT) adapter primer. The RNA template was removed by digestion with RNase H, and the cDNA was then diluted 10-fold for amplification by PCR using three different *pho84*-specific forward primers (5′-CTGTTGGCGTTGGTTGCTCG; 5′-CGTGGTACTGCTCATGG; and 5′-GATAGCAAGTGGAAGAGCTG) and an abridged universal reverse primer. The PCR products were gel-purified and cloned into a pCRII TOPO vector by using the TOPO TA cloning kit (Invitrogen). Plasmid DNAs isolated from individual bacterial transformant colonies were sequenced. cDNAs were deemed to be "independent" when they contained different lengths of poly(dA) at the cloning junction.

DNA binding by EMSA

^{32}P-Labeled DNA fragments were generated by PCR amplification of *pho84* promoter segments using 5′ ^{32}P-labeled forward primers (prepared with [γ-^{32}P]ATP and T4 polynucleotide kinase and then separated from [γ-^{32}P]ATP by Sephadex G-25 gel filtration) and non-labeled reverse primers. The PCR fragments were purified by electrophoresis through a native 8% polyacrylamide gel in 1× TBE buffer (80 mM Tris borate, 1.2 mM EDTA, 2.5% glycerol), eluted from an excised gel slice, ethanol-precipitated, and resuspended in 10 mM Tris-HCl, pH 8.0, 1 mM EDTA at a concentration of 0.25 μM. EMSA reaction mixtures (10 μl) containing 50 mM Tris-HCl, pH 7.4, 10% glycerol, 340 ng of poly(dI-dC) (Sigma), 0.05 pmol of ^{32}P-labeled DNA, and 2 μl of Pho7-DBD (purified as described in Ref. 10) and serially diluted in buffer containing 50 mM Tris-HCl, pH 7.5, 250 mM NaCl, 10% glycerol, 0.1% Triton X-100) were incubated for 10 min at room temperature. The mixtures were analyzed by electrophoresis through a native 6% polyacrylamide gel containing 2.5% (v/v) glycerol in 0.25× TBE buffer. ^{32}P-Labeled DNAs (free and Pho7-bound) were visualized by autoradiography.

DNase I footprinting

^{32}P-Labeled DNA fragments of the *pho84* promoter were generated by PCR amplification and purified as described above, using either a 5′ ^{32}P-labeled forward primer and non-labeled reverse primer (to label the top strand) or a 5′ ^{32}P-labeled reverse primer and non-labeled forward primer (to label the bottom strand). Footprinting reaction mixtures (10 μl) containing 50 mM Tris-HCl, pH 7.4, 10% glycerol, and ^{32}P-labeled DNA and Pho7-DBD as specified were incubated for 10 min at room temperature. The mixtures were then adjusted to 2.5 mM $MgCl_2$ and 0.5 mM $CaCl_2$ and reacted with 0.01 units of DNase I (New England Biolabs) for 90 s at room temperature. The DNase I reaction was quenched by adding 200 μl of STOP solution (50 mM sodium acetate, pH 5.2, 1 mM EDTA, 0.1% SDS, 30 μg/ml yeast tRNA). The mixture was phenol/chloroform-extracted, ethanol-precipitated, and resuspended in 90% formamide, 50 mM EDTA. The samples were heated at 95 °C and then analyzed by urea-PAGE. ^{32}P-Labeled DNAs were visualized by autoradiography.

Author contributions—A. G., A. M. S., S. S., and B. S. conceptualization; A. G., A. M. S., S. S., and B. S. formal analysis; A. G., A. M. S., S. S., and B. S. investigation; A. G., A. M. S., S. S., and B. S. writing-review and editing; S. S. and B. S. supervision; S. S. and B. S. funding acquisition; S. S. writing-original draft; S. S. and B. S. project administration.

References

1. Tomar, P., and Sinha, H. (2014) Conservation of PHO pathway in ascomycetes and the role of Pho84. *J. Biosci.* **39,** 525–536 CrossRef Medline
2. Carter-O'Connell, I., Peel, M. T., Wykoff, D. D., and O'Shea, E. K. (2012) Genome-wide characterization of the phosphate starvation response in *Schizosaccharomyces pombe*. *BMC Genomics* **13,** 697 CrossRef Medline
3. Lee, N. N., Chalamcharla, V. R., Reyes-Turcu, F., Mehta, S., Zofall, M., Balachandran, V., Dhakshnamoorthy, J., Taneja, N., Yamanaka, S., Zhou, M., and Grewal, S. I. (2013) Mtr4-like protein coordinates nuclear RNA

processing for heterochromatin assembly and for telomere maintenance. *Cell* **155,** 1061–1074 CrossRef Medline
4. Shah, S., Wittmann, S., Kilchert, C., and Vasiljeva, L. (2014) lncRNA recruits RNAi and the exosome to dynamically regulate *pho1* expression in response to phosphate levels in fission yeast. *Genes Dev.* **28**, 231–244 CrossRef Medline
5. Schwer, B., Sanchez, A. M., and Shuman, S. (2015) RNA polymerase II CTD phospho-sites Ser5 and Ser7 govern phosphate homeostasis in fission yeast. *RNA* **21,** 1770–1780 CrossRef Medline
6. Chatterjee, D., Sanchez, A. M., Goldgur, Y., Shuman, S., and Schwer, B. (2016) Transcription of lncRNAprt, clustered prt RNA sites for Mmi1 binding, and RNA polymerase II CTD phospho-sites govern the repression of pho1 gene expression under phosphate-replete conditions in fission yeast. *RNA* **22,** 1011–1025 CrossRef Medline
7. Ard, R., Tong, P., and Allshire, R. C. (2014) Long non-coding RNA-mediate transcriptional interference of a permease gene confers drug tolerance in fission yeast. *Nat. Commun.* **5,** 5576 CrossRef Medline
8. Sanchez, A. M., Shuman, S., and Schwer, B. (2018) Poly(A) site choice and pol II CTD Serine-5 status govern lncRNA control of phosphate-responsive tgp1 gene expression in fission yeast. *RNA* **24,** 237–250 CrossRef Medline
9. Henry, T. C., Power, J. E., Kerwin, C. L., Mohammed, A., Weissman, J. S., Cameron, D. M., and Wykoff, D. D. (2011) Systematic screen of *Schizosaccharomyces pombe* deletion collection uncovers parallel evolution of the phosphate signal pathways in yeasts. *Eukaryot. Cell* **10,** 198–206 CrossRef Medline
10. Schwer, B., Sanchez, A. M., Garg, A., Chatterjee, D., and Shuman, S. (2017) Defining the DNA binding site recognized by the fission yeast Zn_2Cys_6 transcription factor Pho7 and its role in phosphate homeostasis. *mBio* **8,** e01218-17 CrossRef Medline
11. Rhind, N., Chen, Z., Yassour, M., Thompson, D. A., Haas, B. J., Habib, N., Wapinski, I., Roy, S., Lin, M. F., Heiman, D. I., Young, S. K., Furuya, K., Guo, Y., Pidoux, A., Chen, H. M., *et al.* (2011) Comparative functional genomics of the fission yeasts. *Science* **332,** 930–936 CrossRef Medline
12. Gunaratne, J., Schmidt, A., Quandt, A., Neo, S. P., Saraç, O. S., Gracia, T., Loguercio, S., Ahrné, E., Xia, R. L., Tan, K. H., Lössner, C., Bähler, J., Beyer, A., Blackstock, W., and Aebersold, R. (2013) Extensive mass spectrometry-based analysis of the fission yeast proteome. *Mol. Cell. Proteomics* **12,** 1741–1751 CrossRef Medline
13. Carpy, A., Krug, K., Graf, S., Koch, A., Popic, S., Hauf, S., and Macek, B. (2014) Absolute proteome and phosphoproteome dynamics during the cell cycle of *Schizosaccharomyces pombe* (fission yeast). *Mol. Cell. Proteomics* **13,** 1925–1936 CrossRef Medline
14. Lemay, J. F., Larochelle, M., Marguerat, S., Atkinson, S., Bähler, J., and Bachand, F. (2014) The RNA exosome promotes transcription termination of backtracked RNA polymerase II. *Nat. Struct. Mol. Biol.* **21,** 919–926 CrossRef Medline
15. Chalamcharla, V. R., Folco, H. D., Dhakshnamoorthy, J., and Grewal, S. I. (2015) Conserved factor Dhp1/Rat1/Xrn2 triggers premature transcription termination and nucleates heterochromatin to promote gene silencing. *Proc. Natl. Acad. Sci. U.S.A.* **112,** 15548–15555 CrossRef Medline
16. Touat-Todeschini, L., Shichino, Y., Dangin, M., Thierry-Mieg, N., Gilquin, B., Hiriart, E., Sachidanandam, R., Lambert, E., Brettschneider, J., Reuter, M., Kadlec, J., Pillai, R., Yamashita, A., Yamamoto, M., and Verdel, A. (2017) Selective termination of lncRNA transcription promotes heterochromatin silencing and cell differentiation. *EMBO J.* **36,** 2626–2641 CrossRef Medline
17. Mata, J. (2013) Genome-wide mapping of polyadenylation sites in fission yeast reveals widespread alternative polyadenylation. *RNA Biol.* **10,** 1407–1414 CrossRef Medline
18. Loya, T. J., and Reines, D. (2016) Recent advances in understanding transcription termination by RNA polymerase II. *F1000Res.* 2016 **5,** 1478 CrossRef Medline
19. Witt, I., Straub, N., Käufer, N. F., and Gross, T. (1993) The CAGTCACA box in the fission yeast *Schizosaccharomyces pombe* functions like a TATA element and binds a novel factor. *EMBO J.* **12,** 1201–1208 Medline
20. Witt, I., Kwart, M., Gross, T., and Käufer, N. F. (1995) The tandem repeat AGGGTAGGGT is, in the fission yeast, a proximal activation sequence and activates basal transcription mediate by the sequence TGTGACTG. *Nucleic Acids Res.* **23,** 4296–4302 CrossRef Medline
21. Gross, T., and Käufer, N. F. (1998) Cytoplasmic ribosomal protein genes of the fission yeast *Schizosaccharomyces pombe* display a unique promoter type: a suggestion for nomenclature of cytoplasmic ribosomal proteins in databases. *Nucleic Acids Res.* **26,** 3319–3322 Medline
22. Schwer, B., Bitton, D. A., Sanchez, A. M., Bähler, J., and Shuman, S. (2014) Individual letters of the RNA polymerase II CTD code govern distinct gene expression programs in fission yeast. *Proc. Natl. Acad. Sci. U.S.A.* **111,** 4185–4190 CrossRef Medline
23. Schwer, B., and Shuman, S. (2011) Deciphering the RNA polymerase II CTD code in fission yeast. *Mol. Cell* **43,** 311–318 CrossRef Medline
24. Schwer, B., Sanchez, A. M., and Shuman, S. (2012) Punctuation and syntax of the RNA polymerase II CTD code in fission yeast. *Proc. Natl. Acad. Sci. U.S.A.* **109,** 18024–18029 CrossRef Medline
25. Estill, M., Kerwin-Iosue, C. L., and Wykoff, D. D. (2015) Dissection of the PHO pathway in *Schizosaccharomyces pombe* using epistasis and the alternate repressor adenine. *Curr. Genet.* **61,** 175–183 CrossRef Medline
26. Herrick, D., Parker, R., and Jacobson, A. (1990) Identification and comparison of stable and unstable RNAs in *Saccharomyces cerevisiae*. *Mol. Cell. Biol.* **10,** 2269–2284 CrossRef Medline
27. Schwer, B., Mao, X., and Shuman, S. (1998) Accelerated mRNA decay in conditional mutants of yeast mRNA capping enzyme. *Nucleic Acids Res.* **26,** 2050–2057 CrossRef Medline